2. Larger Benthic Foraminifers of the Marion Plateau, Northeastern Australia (ODP Leg 194): Comparison of Faunas from Bryozoan (Sites 1193 and 1194) and Red Algal (Sites 1196–1198) Dominated Carbonate Platforms[1]

Pamela Hallock,[2] Kathryn Sheps,[2] George Chaproníère,[3] and Michael Howell[2]

ABSTRACT

Two Neogene carbonate platforms on the Marion Plateau, off northeastern Australia, were drilled during Ocean Drilling Program Leg 194. Approximately 510 m of mixed shelf and slope sediments were penetrated at Site 1193, and ~672 m of shallow-water platform sediments were penetrated at Site 1196. Shallow-water carbonates at Site 1193 were dominated by bryozoans. At Site 1196, coralline red algae dominated, though stony corals were common to abundant in some intervals. Larger benthic foraminifers (LBF) were abundant at both sites, with common genera including *Amphistegina, Cycloclypeus, Lepidocyclina, Miogypsina,* and *Operculina.*

Five LBF assemblages were distinguished using thin sections cut from recovered cores. Assemblage A was found in mixed carbonate-terrigenous clastic neritic facies (<100 m) associated with basement flooding. *Operculina complanata* was common in terrigenous mud-rich facies, whereas *Lepidocyclina* spp. with relatively primitive, nonstellate morphologies dominated in more carbonate-rich facies. These taxa are characteristic of larger foraminiferal (LF) Associations 1–5, indicative of

latest Oligocene to early Miocene ages. Nannofossil dates are similar (~18–24 Ma) for the units immediately above basement. Depositional environments ranged from deltaic muds with oyster and *Operculina* shells to a striking interval of in situ, large, flat *Lepidocyclina badjirraensis* at Site 1198, indicating a deep oligophotic (~100–150 m) paleoenvironment. Assemblage B was found in platform facies at Sites 1193 and 1196 and in corresponding slope sediments at Sites 1197 and 1198. This assemblage is characterized by predominantly nonstellate lepidocyclinids and ovate miogypsinids. Units containing this assemblage are interpreted to be late early Miocene (~16–18 Ma) and indicate deposition in a range of euphotic paleodepths, as interpreted from LBF morphologies. Assemblage C, found at Site 1196 (183–326 meters below seafloor), is characterized by *Flosculinella, Austrotrillina,* soritids, and smaller miliolid foraminifers. This LF 8 association is considered middle Miocene (~13.3–15.2 Ma), an assumption consistent with nannofossil dates from the interval. The assemblage and associated sediments indicate shallow (<12 m), somewhat restricted platform conditions, including seagrass meadows. Assemblage D was found in platform facies at Sites 1193, 1194, and 1196 and in corresponding slope sediments at Sites 1197 and 1198. This assemblage is characterized by the transition from mixed concentric and stellate lepidocyclinid morphologies to predominantly stellate forms, as well as by vermiform miogypsinids. Units containing this assemblage are interpreted to be middle Miocene (~11.9–16.4 Ma). At Sites 1193 and 1194, the middle Miocene regression is recorded by changes in foraminiferal taxa and LBF morphologies. Assemblage E was found in upper platform facies at Site 1196, in corresponding periplatform sediments at Sites 1197 and 1198, and also in transported sediments at Sites 1193 and 1194. *Amphistegina* dominated this assemblage, with stellate *Lepidocyclina* as a common component. Nannofossil and planktonic foraminiferal biostratigraphy in periplatform sediments indicate a late Miocene to earliest Pliocene age for this assemblage.

The cool–subtropical climate was critical to the depositional history of the Marion Plateau throughout the Miocene. Fluvial input, ocean currents, and paleochemistry played critical roles in inhibiting reef development on the northern platform while promoting it on the southern platform. On the southern platform, strong, warm, southward-flowing currents favored coralline algal dominance. Behind the coralline algal rim, coralline algae, stony corals, and LBF thrived. The carbonate factory on the southern platform kept pace with sea level pulses throughout the Miocene, most dramatically during the early middle Miocene when miliolid LBF indicate 180 m of shallow (<12 m) restricted platform sedimentation. Shallow-water carbonate sedimentation on the southern platform terminated in the late Miocene or early Pliocene, and strong currents over the platform have precluded subsequent pelagic sedimentation.

INTRODUCTION

Marion Plateau carbonate platforms and adjacent slopes (Fig. F1) were drilled during Ocean Drilling Program Leg 194; objectives included calibrating the magnitude of Miocene sea level changes and elucidating development of subtropical carbonate platforms in current-dominated environments (Shipboard Scientific Party, 2002). The original working hypothesis was that the northern platform (Site 1193) de-

F1. Marion Plateau and drill sites, p. 13.
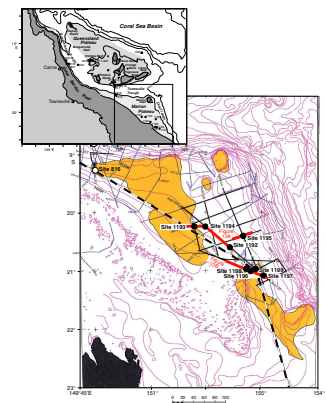
veloped in the early to middle Miocene, whereas the southern platform represented late Miocene development (Pigram et al., 1992).

Shipboard analyses of cores, core catcher samples, and thin sections by the Leg 194 Shipboard Scientific Party (2002) revealed contrasting cool–subtropical carbonate platform facies at Sites 1193 and 1196. Platform facies at Site 1193 (Fig. F2) are dominated by bryozoans and coralline algae with abundant larger benthic foraminifers (LBF). Facies at Site 1196 (Fig. F3) are dominated by coralline red algae, with LBF and hermatypic corals abundant in some intervals. Both nannofossils and LBF provided biostratigraphic evidence that most of the southern platform developed before or during the middle Miocene (Shipboard Scientific Party, 2002), indicating that most differences in platform development are related to paleoenvironmental rather than temporal differences.

LBF assemblages provided crucial data for interpretation of the biostratigraphy, depositional environments, and sea level history of Marion Plateau carbonate platforms during shipboard analysis of cores retrieved during Leg 194 (Shipboard Scientific Party, 2002). LBF were common constituents not only in most platform sediments, but also in periplatform deposits in slope facies. Miocene LBF have been widely studied in Australia and southeast Asia; therefore, biofacies and ranges of many taxa are relatively well known (Chapronière, 1980, 1981, 1984; Betzler and Chapronière, 1993; Chapronière and Betzler, 1993; Betzler, 1997). Assemblages, morphologies, mineralogies, and abundances of LBF also provide clues to paleoenvironmental conditions, including paleodepth, temperature, carbonate saturation state, nutrient supply, light, and water motion, all of which are critical to understanding sea level amplitudes, platform depositional environments, and paleoceanographic history of the sites and intervals sampled. The purpose of this paper is to summarize biostratigraphic and paleoenvironmental interpretations based upon LBF assemblages found at Sites 1193–1198, with the goal of contributing to understanding the depositional history of the Marion Plateau.

METHODS

Thin sections, prepared shipboard during Leg 194 and subsequently from shipboard-requested samples, were examined with the goal of comparing assemblages between platforms. LBF were identified using petrographic optical microscopy based upon previously published criteria (Cole, 1954, 1957a, 1957b, 1963; Chapronière, 1980, 1981, 1984; Betzler, 1997; others). Data collection included identification of LBF and selected associated smaller foraminifers and paleoenvironmental interpretation based on foraminiferal assemblages (Chapronière, 1975, 1981; Betzler and Chapronière, 1993), LBF shapes and mineralogies (e.g., Hallock and Glenn, 1986; Hallock, 1999), and other available sedimentological data (Shipboard Scientific Party, 2002). Biostratigraphic analyses included interpreting ages of assemblages using age ranges of key taxa from the literature and by utilizing planktonic foraminiferal and nannofossil ages from Leg 194 cores (Shipboard Scientific Party, 2002). Paleoenvironmental analyses included comparing the LBF assemblages with existing models (e.g., Hallock and Glenn, 1986; Betzler and Chapronière, 1993; Hottinger, 1997; Hallock, 1999; Hohenegger, 1999; others).

F2. Northern platform seismic correlation, p. 14.
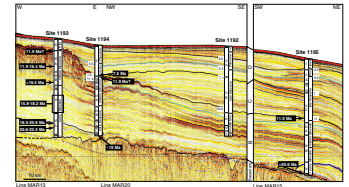
F3. Southern platform seismic correlation, p. 15.
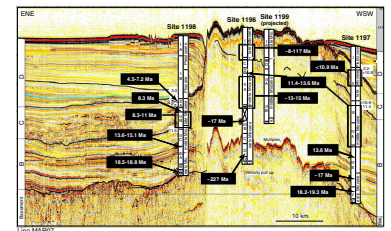
Deposition Following Basement Flooding

Basement volcanics, or terrigenous sediments and larger clasts interpreted as near basement, were reached at Sites 1193, 1194, 1197, and 1198 (Shipboard Scientific Party, 2002). LBF (Figs. F4, F5, F6) occurred in inundation sequences above acoustic basement in sediments ranging from meters-thick, oyster-rich muds containing *Operculina complanata* (Defrance) (Fig. F4) that graded into more carbonate-rich facies at Sites 1193 (Fig. F5A) and 1197 (Fig. F6C), to a few centimeters of LBF-rich sediments lying between basement and overlying pelagic units at Sites 1194 (421 meters below seafloor [mbsf]) (Fig. F5D) and 1198 (506 mbsf) (Fig. F6D). Although basement was not reached at Site 1196, the sediments in the deepest interval penetrated (643–672 mbsf) were dark sandstones with *O. complanata* as a biotic component. The oldest sediments retrieved at Site 1195 (517 mbsf) also contained a diverse LBF assemblage (Fig. F5B).

The oldest LBF assemblages encountered are characteristic of latest Oligocene and earliest Miocene (~24–20 Ma) LF associations (LF 1–3), which have been previously described from Australia and New Zealand by Chaproniére (1975, 1980, 1984). This range is consistent with nannofossil ages available for the bases of these cores (Shipboard Scientific Party, 2002). Characteristic LBF taxa (Figs. F4, F5, F6) include *Amphistegina bikiniensis* (Todd and Post), *Lepidocyclina* (*Eulepidina*) *ephippioides* (Jones and Chapman), *Lepidocyclina* (*Nephrolepidina*) *sumatrensis* (Brady), and *O. complanata* (Chaproniére, 1981). Arrangements of equatorial chambers in *Lepidocyclina* (*Nephrolepidina*) indicate relatively primitive circular-concentric patterns (i.e., nonstellate morphologies) as indicated by Chaproniére's (1980, 1981) F-parameter values <2, which are also indicative of latest Oligocene to early Miocene age.

At Site 1193, ~100 m of mixed siliciclastics and carbonates, biotically characterized by bryozoans and LBF representing LF 1–3 assemblages, were penetrated. Samples 194-1193A-75X-CC (456 mbsf) through 83X-CC (513 mbsf) and 194-1193C-5X-CC (515 mbsf) through 8X-CC (544 mbsf) include both coarse bioclastic and terrigenous clastic sediments, the latter generally increasing downhole (Shipboard Scientific Party, 2002). The LBF assemblages indicate inner to middle neritic water depths for most of this interval. Reworked glauconite and phosphate-infilled bioclasts are common (Fig. F5A, F5C). Nannofossils constrain the age of this interval to 23–18 Ma (Shipboard Scientific Party, 2002), indicating that the cumulative deposition rate was on the order of 20 m/m.y. This interval also represents seismically defined Megasequence A (Shipboard Scientific Party, 2002). A 50-m interval of similar glauconite- and phosphate-infilled bioclasts, including LBF (Fig. F5B), was also found just above basement at Site 1197. Nannofossils indicated age as ~18–19 Ma (Shipboard Scientific Party, 2002).

Deposition During the Late Early Miocene Sea Level Rise

Following deposition of an interval of arkosic sandstone at ~450–430 mbsf (base of seismic Megasequence B) (Fig. F2), carbonate deposition at Site 1193 abruptly increased as siliciclastic input declined. Nannofossils date this change at ~18.5 Ma. Bryozoan and LBF components increase uphole as percent carbonate increases, with imbricated grainstones and packstones (Fig. F7) dominated by *Lepidocyclina (Nephrolepidina) praehowchini* (Chaproniére) and diverse other LBF (LF 6 of

F4. Bioclastic debris, ~22.5 Ma, p. 16.
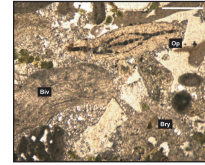
F5. Representative LBF, >20.6 Ma p. 17.
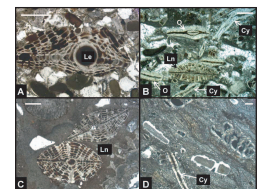
F6. Representative LBF, Southern Marion Platform, p. 18.
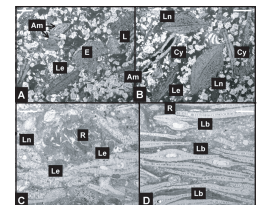
F7. Representative LBF, 16.8–18.2 Ma p. 19.
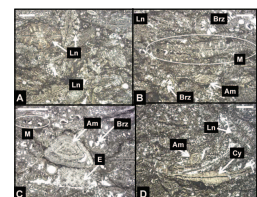
Chaproinère [1981]) found at 390 mbsf at the top of lithologic Unit VI (Fig. F2). The continued prevalence of nonstellate lepidocyclinid morphologies (F-parameter < 2.5) is indicative of early Miocene deposition (Chaproinère, 1980, 1981).

Evidence of increasing paleodepth at ~18 Ma is seen at all the sites, except Site 1196. At Site 1193, imbricated lepidocyclinid grainstones are succeeded by >150 m of calcareous silt and very fine carbonate sands with bioclastic fragments (Fig. F8), as well as foraminiferal assemblages that indicate deposition at subeuphotic, probably outer neritic depths (>150 m) for ~23 m.y. An accumulation rate of >50 m/m.y. indicates active upslope production, downslope transport, and deposition at this location. At Sites 1194, 1195, and 1198, LBF-rich grainstones or packstones immediately above basement are overlain by similar very fine bioclastic carbonates. Although the basal shallow-water sequence is thicker at Site 1197, it too is abruptly overlain by fine-grained carbonates (~600 mbsf).

Rapid inundation is particularly evident at Site 1198, where a red algal/foraminiferal boundstone consisting of large, very thin foraminifers bound by thin red algal crusts (Fig. F6D) lies upon olivine basalt at 513 mbsf. The carbonate unit is topped by a phosphatic hardground. The LBF assemblage is dominated by *L. (E.) badjirraensis* and *Cycloclypeus eidae,* which are the characteristic taxa of LF 5 (Chaproinère, 1981, 1984), again indicating deposition in the early Miocene (~18–19 Ma).

At Site 1196, the rapid rise in sea level in the late early Miocene did not overwhelm shallow-water carbonate deposition dominated by red algae, stony coral, and LBF. Rather, combined with subsidence, sea level rise provided accommodation space for accumulation of ~300 m of shallow-water carbonates through the early Miocene (Fig. F3). One calcareous nannofossil date of 24.6–24.2 Ma in Sample 194-1196A-70R-1, 133 cm (664 mbsf), in apparently deltaic facies (Shipboard Scientific Party, 2002), constrains the maximum age of the platform. Extensive dolomitization severely limits biostratigraphic and paleoenvironmental interpretation of most of the interval between ~330 and 620 mbsf. However, a *Miogypsina*-rich facies at 383–393 mbsf (Fig. F9A, F9B) has a very similar assemblage to that seen at 340 mbsf at Site 1193 (Fig. F7), as well as in transported sediments in Samples 194-1197B-53R-5, 92 cm (557 mbsf) (Fig. F9C), and 194-1198B-26R-5, 48 cm (443 mbsf) (Fig. F9D).

ACCRETION OF CARBONATE PLATFORMS DURING THE MIDDLE MIOCENE

Regression in the middle Miocene returned Site 1193 into the euphotic zone. Subsequently, 200 m of limestones and dolostones accumulated (Fig. F2), dominated by bryozoans and LBF whose sizes and shapes indicate paleodepths ranging from oligophotic (>50 m; terminology of Pomar [2001]) to shallow euphotic (<30 m). Common occurrences of large, relatively delicate lepidocyclinids (Fig. F10A) and of large, flat *Cycloclypeus* (Fig. F10B) between 100 and 223 mbsf indicate relatively oligophotic conditions, probably on the order of 50–100 m. Between 40 and 90 mbsf, robust morphologies of LBF and evidence for physical damage to skeletal material (Fig. F10C, F10D) indicate shallower conditions (<30 m), which is consistent with several exposure surfaces that

F8. Bioclastic debris, ~16.4 Ma, p. 20.
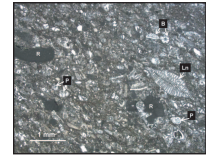
F9. Early to early middle Miocene LBF-rich facies, p. 21.
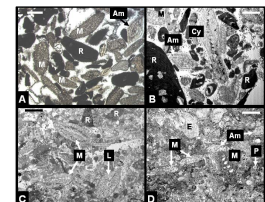
F10. Middle Miocene LBF-rich facies, p. 22.
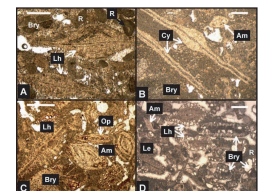
have been interpreted in this interval (Shipboard Scientific Party, 2002). Stellate morphologies of *Lepidocyclina* become increasingly prevalent uphole (F-parameter = 3–4), indicating a middle Miocene LBF assemblage (Chapronière, 1981). Other notable LBF include vermiform *Miogypsina thecideaeformis* (Rutten). The upper few meters (at least 36.6–37.9 mbsf) of the "platform" is characterized by reworked benthic material and exposure surfaces (Shipboard Scientific Party, 2002), whose interpretation is complicated by bioerosion during late Miocene drowning of platform facies.

Site 1194 corroborates the story of early Miocene sea level rise and middle Miocene sea level fall interpreted at Site 1193. Following early Miocene submergence (>18.2 Ma from nannofossil dates; Shipboard Scientific Party, 2002), >100 m of carbonates accumulated (264–375 mbsf) consisting of very fine bioclastics and planktonic foraminifers. The presence of outer neritic to upper bathyal benthic foraminifers indicate the deepest paleoenvironment for this site during the early and middle Miocene. At 256 mbsf, bioclastic debris, particularly bryozoan fragments, increase in size, whereas planktonic foraminifers become less dominant, indicating a shift to neritic conditions (Shipboard Scientific Party, 2002). Shoaling continues upward; at 158 m, *Amphistegina* spp. become abundant, indicating either euphotic depths or transport from euphotic depths in the interval between 115 and 158 mbsf. In Samples 194-1194A-16X-CC (132.9 mbsf) and 194-1194B-4R-CC (138.8 mbsf), abundant specimens of modern-appearing *Amphistegina lessonii* (d'Orbigny) that are normal in size (1–2 mm diameter) and intermediate in thickness, along with common *Amphistegina radiata* (Fichtel and Moll) and *Operculina* (Fig. F11), indicate water depths of ~30–50 m. Nannofossils indicate the age of this lowstand interval at between 11.9 and 13.6 Ma (Shipboard Scientific Party, 2002).

As noted previously, much of the history of Site 1196 is lost to poor core recovery and dolomitization. Nevertheless, deposition contrasts with that at Site 1193 by the striking differences in dominant macrobiota. Bryozoans dominate shallow-water carbonate sediments at Site 1193 (e.g., Fig. F10D), with red algae and LBF generally of secondary importance. Red algal fragments and rhodoliths dominate sediments at Site 1196, with corals and LBF generally of secondary importance and bryozoans relatively rare (Shipboard Scientific Party, 2002). Thus, photosynthetically driven calcification was the dominant process at Site 1196, whereas heterozoan (terminology of James, 1997) calcification was dominant at Site 1193, even though the widespread presence of LBF indicates that much of the deposition at Site 1193 occurred within the photic zone. The difference between photozoan calcification and heterozoan calcification probably accounts for why sedimentation at Site 1196 kept pace with late–early Miocene sea level rise, whereas sedimentation at Site 1193 did not.

Despite differences in dominant macrobiota between the platforms, LBF assemblages were generally similar (Figs. F7, F9, F10). One remarkable environmentally induced (facies) difference was found in lithologic Subunit IIA (Shipboard Scientific Party, 2002) at Site 1196 between 182 and 336 mbsf. In this interval of skeletal floatstones and grainstones, both large and small porcelaneous foraminifers (Fig. F12) dominate the assemblage, indicating warm shallow waters with higher carbonate saturation than any other interval seen at any site during Leg 194. The presence of visible bits of organic matter, probably remains of seagrasses, along with abundant gastropods and bivalves (Figs. F12A, F12B) (Shipboard Scientific Party, 2002), corroborate the interpretation

F11. Assemblage at ~30–50 m paleodepth, p. 23.
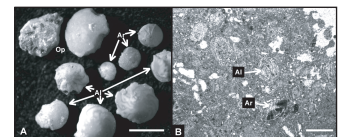
F12. Distinctive foraminifers, p. 24.
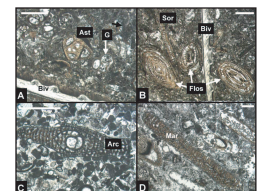
that environmental conditions remained near sea level (<12 m). *Austrotrillina howchini* and *Flosculinella botangensis* (Fig. F12A, F12B) are abundant in this interval; these species characterize Chapronière's (1981) middle Miocene LF 8 assemblage, interpreted as 13.3–15.2 Ma. Nannofossil dates of 13.6–18.2 Ma for two samples within this interval are consistent with the LBF ranges. The thickness, age, and distinctly shallow-water nature of this interval of sedimentation indicates that the combined effects of sea level rise and subsidence provided 150 m of accommodation space in ~2 m.y. and that platform accretion kept pace. Probable exposure surfaces above this interval (Shipboard Scientific Party, 2002) suggest that this facies preceded the late middle Miocene regression.

Meanwhile, deposition at offbank Sites 1197 and 1198 was dominated by planktonic foraminifers and bioclastic calcareous silts and fine sands, principally red algal in origin, but including larger foraminiferal debris (Fig. F13A, F13B). The interval between Samples 198-1198B-18R-CC and 20R-CC (364–382 mbsf) is dated by nannofossils and planktonic foraminifers at 13.6–15.1 Ma, which is consistent with the LF 8 range of 13.3–15.2 Ma for lithologic Subunit IIA at Site 1196. Furthermore, Sample 194-1196A-19R-1, 1 cm (Subunit ID; Shipboard Scientific Party, 2002), contains a very similar LBF assemblage (Fig. F13C, F13D) to the transported LBF common between 185 and 349 mbsf in Hole 1197B (Fig. F14), which is dated between 11.4 and 13.6 Ma by calcareous nannofossils and planktonic foraminifers (Shipboard Scientific Party, 2002). *Lepidocyclina (Nephrolepidina) howchini* (predominantly stellate) (Chapronière 1981, 1984), *M. thecideaeformis,* and *Operculina* spp. are common to both. *Amphistegina* spp. and *Cycloclypeus* spp., including *Cycloclypeus (Katacycloclypeus) annulatus* (Fig. F14B), also were present in transported sediments at Site 1197.

LATE MIOCENE DEPOSITION

Both planktonic foraminifers and calcareous nannofossils indicate that the interval between ~230 and 330 mbsf at Site 1198 was deposited during the late Miocene (8.3–11 Ma). LBF assemblages (Fig. F15) transported into this interval are dominated by stellate *L. (N.) howchini* and *Amphistegina* spp., with common *Cycloclypeus, Lepidocyclina (Nephrolepidina) martini,* and *Operculina.* Furthermore, the final LBF assemblages in Samples 194-1193A-5H-1, 142 cm (~36 mbsf), 194-1194B-2R-4, 69 cm (~115 mbsf), and 194-1197B-2R-1, 42 cm (~62 mbsf), are remarkably similar (Fig. F16). At all three sites, LBF assemblages are dominated by *Amphistegina* spp. and distinctive stellate *Lepidocyclina* and occur in a matrix of planktonic foraminifers and bioclastic carbonates, indicating offbank deposition of late Miocene material. A nannofossil range of 7.5–8.6 Ma in Sample 194-1194A-13H-CC (117.4 mbsf) in the overlying pelagic sediments support this interpretation.

At Site 1196, platform carbonates above 150 mbsf were rich in LBF, though evidence is mostly preserved as molds in dolomitized intervals. The terminal platform LBF assemblage at Site 1196 (Fig. F17A, F17B) is dominated by *Amphistegina* spp. with abundant *Cycloclypeus* and *Operculina* and common stellate *Lepidocyclina*, which provides minimal biostratigraphic constraint on the timing of the platform drowning. Similarly, downslope deposits of platform sediments at Sites 1197 and 1198 are not definitive. However, at Site 1198, for which the best biostratigraphic record is available, a minor lithologic change (lithologic

F13. Mixed LBF assemblage, p. 25.
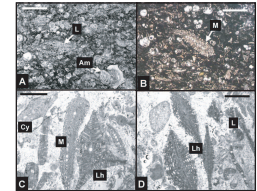
F14. LBF debris in slope sediments, Site 1197, p. 26.
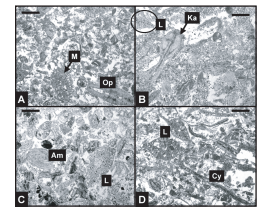
F15. LBF debris in slope sediments, Site 1198, p. 27.
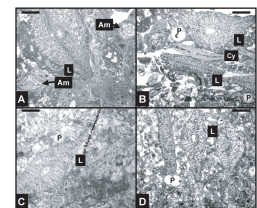
F16. Periplatform sediments, p. 28.
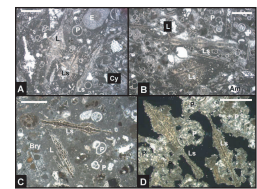
F17. Platform-top and transported sediments, p. 29.
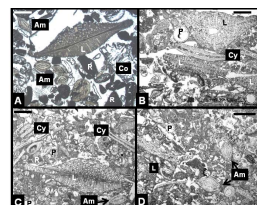
Subunit IIA/IIB boundary; see Shipboard Scientific Party, 2002) was dated at 8.3 Ma, based upon first observation of *Globigerinoides extremus*. Above this boundary, a distinctive lepidocyclinid (Fig. F16C), tentatively identified as *Lepidocyclina (Nephrolepidina) rutteni* (Van der Vlerk), was found, and very similar forms were found in the upper 40 m at Site 1196 (Fig. F16A). Thus, the uppermost MP3 platform was deposited in latest Miocene or earliest Pliocene, consistent with previous observations of *L. (N.) rutteni* on the Queensland Plateau (e.g., Betzler, 1997).

BIOSTRATIGRAPHIC SUMMARY

Cores and thin sections from platform facies at Sites 1193 and 1196 and from associated periplatform sediments at Sites 1194, 1197, and 1198 revealed a continuum of *Lepidocyclina/Amphistegina*-dominated LBF assemblages (Figs. F18, F19). Four assemblages were distinguished using morphologic trends in *Lepidocyclina (Nephrolepidina)* lineages (after Chapronière, 1980) and some notable trends in other taxa. A fifth assemblage represented a distinctly different facies. These assemblages occurred sequentially, indicating temporal stages in platform development. This conclusion is supported by biostratigraphic data provided by nannofossil and planktonic foraminifers (Shipboard Scientific Party, 2002).

Assemblage A, which includes components of Chapronière's (1980, 1981) LF Associations 1–5, was found in a range of neritic facies (<150 m) associated with basement flooding sequences seen at Sites 1193–1197. Nannofossil dates support LBF biostratigraphy, indicating latest Oligocene–early Miocene for basement flooding. *O. complanata* was the dominant LBF in sediments rich in terrigenous muds and oyster fragments. Lepidocyclinids, both *Lepidocyclina (Eulepidina)* spp. and *Lepidocyclina (Nephrolepidina)* spp., were typically the most conspicuous LBF in carbonate facies, whether the dominant biota were bryozoans or red algae. *Lepidocyclina (Nephrolepidina)* spp. were characterized by primitive nonstellate morphologies.

Assemblage B was found in platform facies at Sites 1193 and 1196 and in corresponding slope sediments at Sites 1197 and 1198. This assemblage was characterized by circular-concentric (nonstellate) *Lepidocyclina (Nephrolepidina)* spp., as well as by abundant *Amphistegina, Cycloclypeus,* and *Operculina.* Miogypsinids, when present, were predominantly ovate forms. The predominance of nonstellate *Lepidocyclina (Nephrolepidina)* indicated late–early Miocene deposition, as some stellate morphologies were observed.

Assemblage C, found at Site 1196 (lithologic Subunit IIA at 183–326 mbsf; Shipboard Scientific Party, 2002), was characterized by *Flosculinella, Austrotrillina,* soritids, and smaller miliolid foraminifers. This was biostratigraphically and paleoenvironmentally the most definitive assemblage. Both LBF and nannofossils indicate middle Miocene age. The assemblage was characteristic of very shallow (<12 m), somewhat restricted environmental conditions, including seagrass meadows. Red algal–dominated sediments containing Assemblage B occurred below the Assemblage C interval at Site 1196, whereas red algal and coral facies containing Assemblage D occurred directly above.

Assemblage D is characterized by mixed concentric and stellate morphologies of *Lepidocyclina (Nephrolepidina)* spp., as well as by very modern appearing *Amphistegina* spp. Miogypsinid morphologies were

F18. Drill site correlation, northern platform, p. 30.
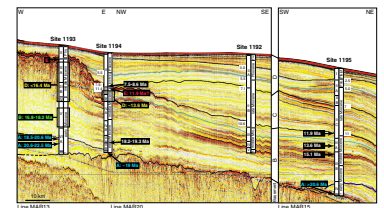
F19. Drill site correlation, southern platform, p. 31.
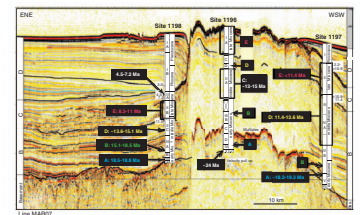
distinctively vermiform, rather than the ovate morphologies seen in Assemblage B. Intervals characterized by this assemblage were interpreted to be middle Miocene in age (Figs. F18, F19).

Assemblage E was found at Site 1196 in the uppermost platform facies and in corresponding periplatform sediments at Sites 1193, 1194, 1197, and 1198. *Amphistegina* spp. dominates the LBF assemblage, although stellate lepidocyclinids were the distinctive component. Planktonic foraminifers and nannofossils indicated that this assemblage occurred in late Miocene (~8–11 Ma) periplatform sediments at Site 1198; overlying pelagic deposition was dated at 7.5–8.6 Ma at Site 1194.

PALEOENVIRONMENTAL SUMMARY

The paleoenvironmental history indicated by the LBF assemblages is even more fascinating. Much remains to be deciphered, though poor core recovery and dolomitization will limit what can be learned. One lesson that is evident in the Leg 194 story is that different photozoan assemblages respond differently to the coralgal "reef" turnon–turnoff gradient (e.g., Buddemeier and Hopley, 1988; Hallock 2001). At Site 1193, LBF occur abundantly in environmental conditions that favor bryozoan dominance of benthic carbonate production. At Site 1196, LBF occur at least as abundantly in coralgal reef facies. The environmental factors that likely controlled Miocene benthic community structure and carbonate sedimentation on the Marion Plateau include temperature, ocean currents, parameters associated with fluvial input, and ocean chemistry.

The cool–subtropical climate was critical to the overall history of the plateau, resulting in environmental conditions that were marginal for coralgal reef development throughout the Miocene. However, temperature differences were not likely to have driven sedimentation differences between the northern and southern platforms. If latitude was involved, the southern platform should have been cooler and therefore bryozoan dominated. Although differences in current regimes around the platforms are poorly known, currents certainly played a key role in the platform history (e.g., John and Mutti, 2005), and not only in transporting the vast drifts of fine terrigenous and calcareous sediments. Moreover, fluvial input, in conjunction with ocean currents and paleochemistry, very likely played the critical role in inhibiting reef development on the northern platform while promoting it on the southern platform.

Hallock (2001) reviewed and discussed the sensitivity of carbonate sedimentation, particularly reef development, to nutrients and carbonate saturation. The benthic communities that produced bryozoan-dominated carbonate facies at Site 1193 likely included abundant fleshy macroalgae and especially filamentous microalgae, which limited recruitment and growth of coralline red algae and stony corals. Pulses of nutrients in terrestrial runoff likely supported the algae and also plankton that provided food for the bryozoans. Nevertheless, the LBF assemblages attest to relatively clear waters with at least cool subtropical (>20°C) paleotemperatures, possibly similar to modern conditions on the west Australian shelf (see James et al., 1999). Conditions on the southern platform (Site 1196) probably included slightly lower fluxes of nutrients and stronger currents, both of which would have increased the competitive advantage of coralline red algae relative to the filamentous algae.

An additional factor that likely influenced overall carbonate production was ocean chemistry, specifically carbonate saturation. The west Australian shelf provides a modern example where photozoan calcite production (i.e., calcite calcification by coralline red algae and LBF) generally dominates over photozoan aragonite production (i.e., aragonite calcification by stony corals and calcareous green algae) (James et al., 1999), indicating that carbonate saturation is below the threshold required for prolific aragonite production (e.g., Kleypas et al., 2001). Where shallow-water conditions allow water to warm and thus increase supersaturation with respect to aragonite (e.g., the Abrolhos Islands off west Australia), carbonate production by calcareous algae and corals can be prolific (Collins et al., 1993, 1997).

The following scenario is proposed to explain platform development and growth on the southern platform of the Marian Plateau. Strong, warm, southward-flowing currents favored coralline algal dominance. Limited upwelling mixed higher-alkalinity waters into surface waters around the platform, thereby promoting calcification. Behind the rapidly accreting coralline algal rim, coralline algae, LBF, and some stony corals thrived. As noted by Hallock (2001), carbonate production rates approach maximum as the reef turn-off threshold is approached. The carbonate factory on the southern platform kept pace with sea level pulses throughout the Miocene, most dramatically during the early middle Miocene when LBF in lithologic Subunit IIA indicate 180 m of shallow (<12 m) platform sedimentation. Higher carbonate saturation on the platform is indicated through this interval by the prevalence of miliolid foraminifers that produced shells of high-Mg calcite.

Leg 194 provided a unique opportunity to examine the Miocene histories of two contemporaneous platforms with very different dominant biota and therefore different accretion potential. Analyses of LBF assemblages recovered during Leg 194 provided crucial biostratigraphic, paleodepth, and paleoceanographic information integral to the success of the project. Determining the seismic and biostratigraphic contexts for the LBF assemblages within the platforms and in associated slope facies has demonstrated that the northern platform accreted in the early and middle Miocene while growth of the southern platform occurred intermittently throughout the Miocene. The abundances of larger benthic foraminifers in both red algal and bryozoan-dominated facies is critical to understanding the nature of Marion Plateau carbonates that might otherwise be interpreted as temperate, based upon limited abundances of zooxanthellate corals and *Halimeda* (e.g., James, 1997).

ACKNOWLEDGMENTS

REFERENCES

Betzler, C., 1997. Ecological control on geometries of carbonate platforms: Miocene/Pliocene shallow-water microfaunas and carbonate biofacies from the Queensland Plateau (NE Australia). *Facies,* 37:147–166.

Betzler, C., and Chapronière, G.C.H., 1993. Paleogene and Neogene larger foraminifers from the Queensland Plateau: biostratigraphy and environmental significance. *In* McKenzie, J.A., Davies, P.J., Palmer-Julson, A., et al., *Proc. ODP, Sci. Results,* 133: College Station, TX (Ocean Drilling Program), 51–66.

Buddemeier, R.W., and Hopley, D., 1988. Turn-ons and turn-offs: causes and mechanisms of the initiation and termination of coral reef growth. *Proc. Int. Coral Reef Symp., 8th,* 1:253–261.

Chapronière, G.C.H., 1975. Palaeoecology of Oligo–Miocene larger foraminiferida, Australia. *Alcheringa,* 1:37–58.

Chapronière, G.C.H., 1980. Biometrical studies of early Neogene larger foraminiferida from Australia and New Zealand. *Alcheringa,* 4:153–181.

Chapronière, G.C.H., 1981. Australasian mid-Tertiary larger foraminiferal associations and their bearing on the East Indian Letter Classification. *BMR J. Aust. Geol. Geophys.,* 6:145–151.

Chapronière, G.C.H., 1984. Oligocene and Miocene larger foraminiferida from Australia and New Zealand. *Bull.—Bur. Miner. Resour., Geol. Geophys. (Aust.),* 188:1–98.

Chapronière, G.C.H., and Betzler, C., 1993. Larger foraminiferal biostratigraphy of Sites 815, 816, and 826, Leg 133, northeastern Australia. *In* McKenzie, J.A., Davies, P.J., Palmer-Julson, A., et al., *Proc. ODP, Sci. Results,* 133: College Station, TX (Ocean Drilling Program), 39–49.

Cole, W.S., 1954. Larger foraminifera and smaller diagnostic foraminifera from Bikini drill holes. *Geol. Surv. Prof. Pap. U.S.,* 260-O:569–608.

Cole, W.S., 1957a. Geology of Saipan Mariana Islands, Part 3. Paleontology, Chapter I. Larger foraminifera. *U.S. Geol. Surv. Prof. Pap.,* 280:321–360.

Cole, W.S., 1957b. Larger foraminifera from the Eniwetok atoll drill holes. *Geol. Surv. Prof. Pap. U.S.,* 260-V:743–784.

Cole, W.S., 1963. Tertiary larger foraminifera from Guam. *U.S. Geol. Surv. Prof. Pap.,* 403:28.

Collins, L.B., France, R.E., Zhu, Z.R., and Wyrwoll, K.-H., 1997. Warm-water platform and cool-watershelf carbonates of the Abrolhos shelf, southwest Australia. *In* James, N.P., and Clarke, J.A.D. (Eds.), *Cool-Water Carbonates.* Spec. Publ.—SEPM (Soc. Sediment. Geol.), 56:23–36.

Collins, L.B., Zhu, Z.R., Wyrwoll, K.-H., Hatcher, B.G., Playford, P.E., Chen, J.H., Eisenhauer, A., and Wasserburg, G.J., 1993. Late Quaternary evolution of coral reefs on a cool-water carbonate margin: the Abrolhos carbonate platforms, southwest Australia. *Mar. Geol.,* 110(3–4):203–212. **doi:10.1016/0025-3227(93)90085-A**

Hallock, P., 1999. Symbiont-bearing foraminifera. *In* Sen Gupta, B.K. (Ed.), *Modern Foraminifera:* Amsterdam (Kluwer), 123–149.

Hallock, P., 2001. Coral reefs, carbonate sedimentation, nutrients, and global change. *In* Stanley, G.D. (Ed.), *The History and Sedimentology of Ancient Reef Ecosystems:* Amsterdam (Kluwer), 387–427.

Hallock, P., and Glenn, E.C., 1986. Large foraminifera: a tool for paleoenvironmental analysis of Cenozoic carbonate depositional facies. *Palaios,* 1(1):55–64.

Hohenegger, J., 1999. Larger foraminifera—microscopical greenhouses indicating shallow-water tropical and subtropical environments in the present and past. *Occas. Pap.— Kagoshima Univ. Res. Cent. Pac. Isl.,* 32:19–45.

Hottinger, L., 1997. Shallow benthic foraminiferal assemblages as signals for depth of their deposition and their limitations. *Bull. Soc. Geol. Fr.,* 168:491–505.

James, N.P., 1997. The cool-water carbonate depositional realm. *In* James, N.P., and Clarke, J.D.A. (Eds.), *Cool-Water Carbonates.* Spec. Publ.—SEPM (Soc. Sediment. Geol.), 56:1–20.

James, N.P., Collins, L.B., Bone, Y., and Hallock, P., 1999. Subtropical carbonates in a temperate realm: modern sediments on the southwest Australian shelf. *J. Sediment. Res.,* 69:1297–1321.

John, C.M., and Mutti, M., 2005. Relative control of paleoceanography, climate, and eustasy over heterozoan carbonates: a perspective from slope sediments of the Marion Plateau (ODP Leg 194). *J. Sediment. Res.,* 75(2):216–230. doi:10.2110/jsr.2005.017

Kleypas, J.A., Buddemeier, R.W., and Gattuso, J.P., 2001. The future of coral reefs in an age of global change. *Int. J. Earth Sci.,* 90(2):426–437. doi:10.1007/s005310000125

Pigram, C.J., Davies, P.J., Feary, D.A., and Symonds, P.A., 1992. Absolute magnitude of the second-order middle to late Miocene sea-level fall, Marion Plateau, Northeast Australia. *Geology,* 20(9):858–862. doi:10.1130/0091-7613(1992)020<0858:AMOTSO>2.3.CO;2

Pomar, L., 2001. Types of carbonate platforms: a genetic approach. *Basin Res.,* 13:313–334. doi:10.1046/j.0950-091x.2001.00152.x

Shipboard Scientific Party, 2002. Leg 194 summary. *In* Isern, A.R., Anselmetti, F.S., Blum, P., et al., *Proc. ODP, Init. Repts.,* 194: College Station TX (Ocean Drilling Program), 1–88. [HTML]

Figure F1. Location of the Marion Plateau relative to northeast Australia and the Great Barrier Reef and ODP Leg 133 and 194 drill sites. Multichannel seismic lines shown in red.
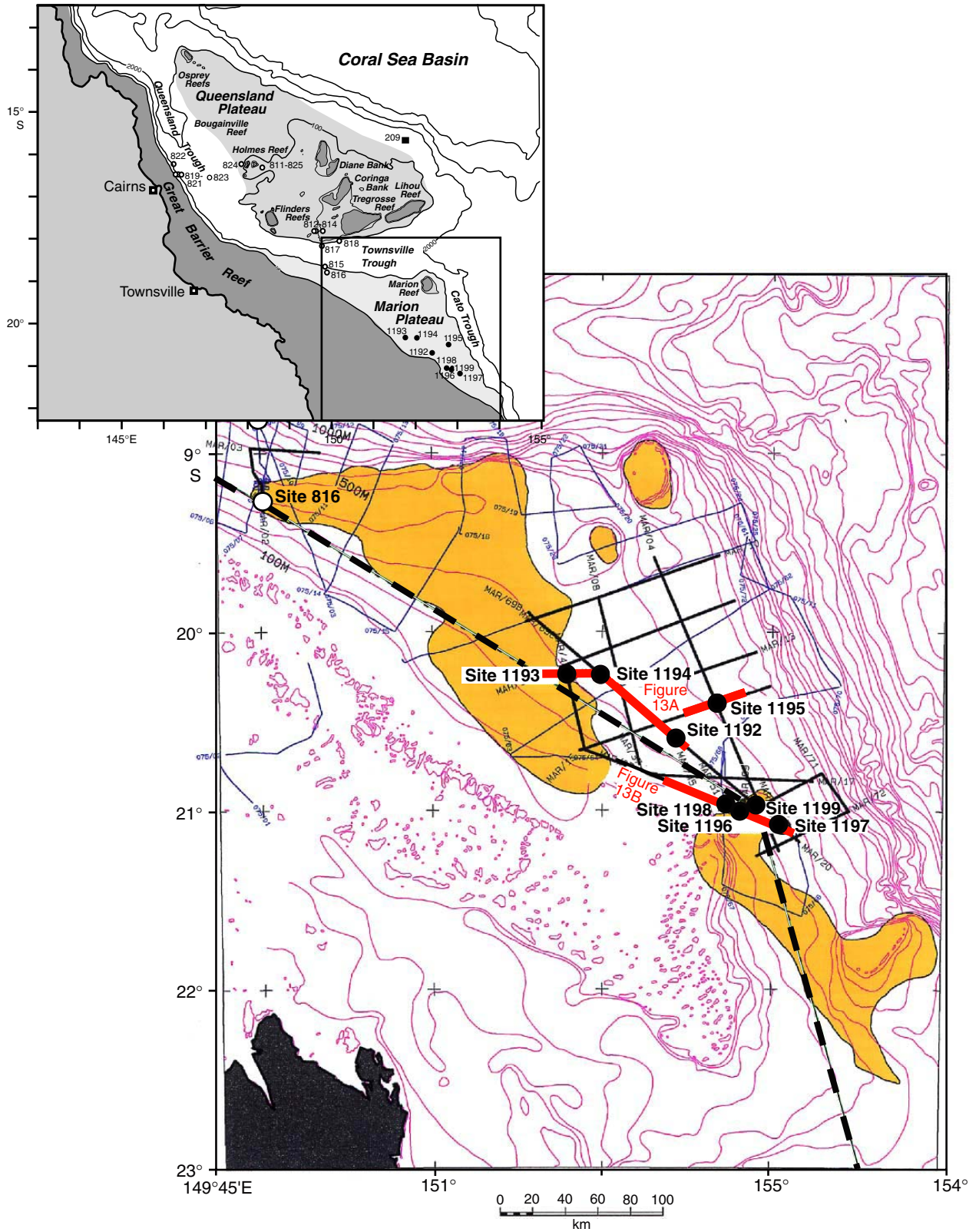
Figure F2. Seismic correlation among Leg 194 drill sites on the northern platform and adjacent slope of the Marion Plateau. Seismically identified megasequences are noted, as are lithologic units and shipboard biostratigraphy (adapted from Shipboard Scientific Party, 2002).
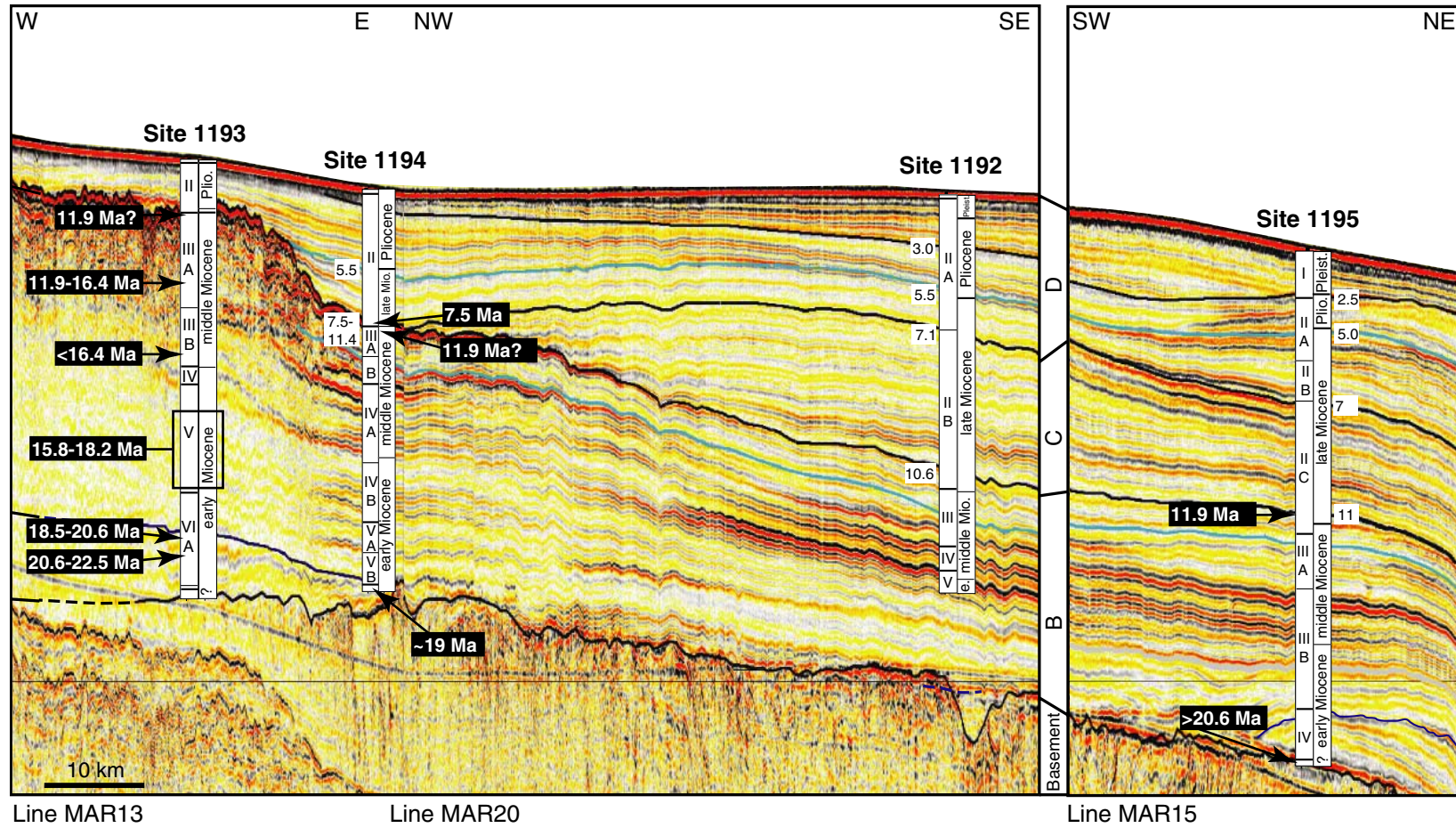
Figure F3. Seismic correlation among Leg 194 drill sites on the southern platform and adjacent slopes of the Marion Plateau. Seismically identified megasequences are noted, as are lithologic units and shipboard biostratigraphy (adapted from Shipboard Scientific Party, 2002).
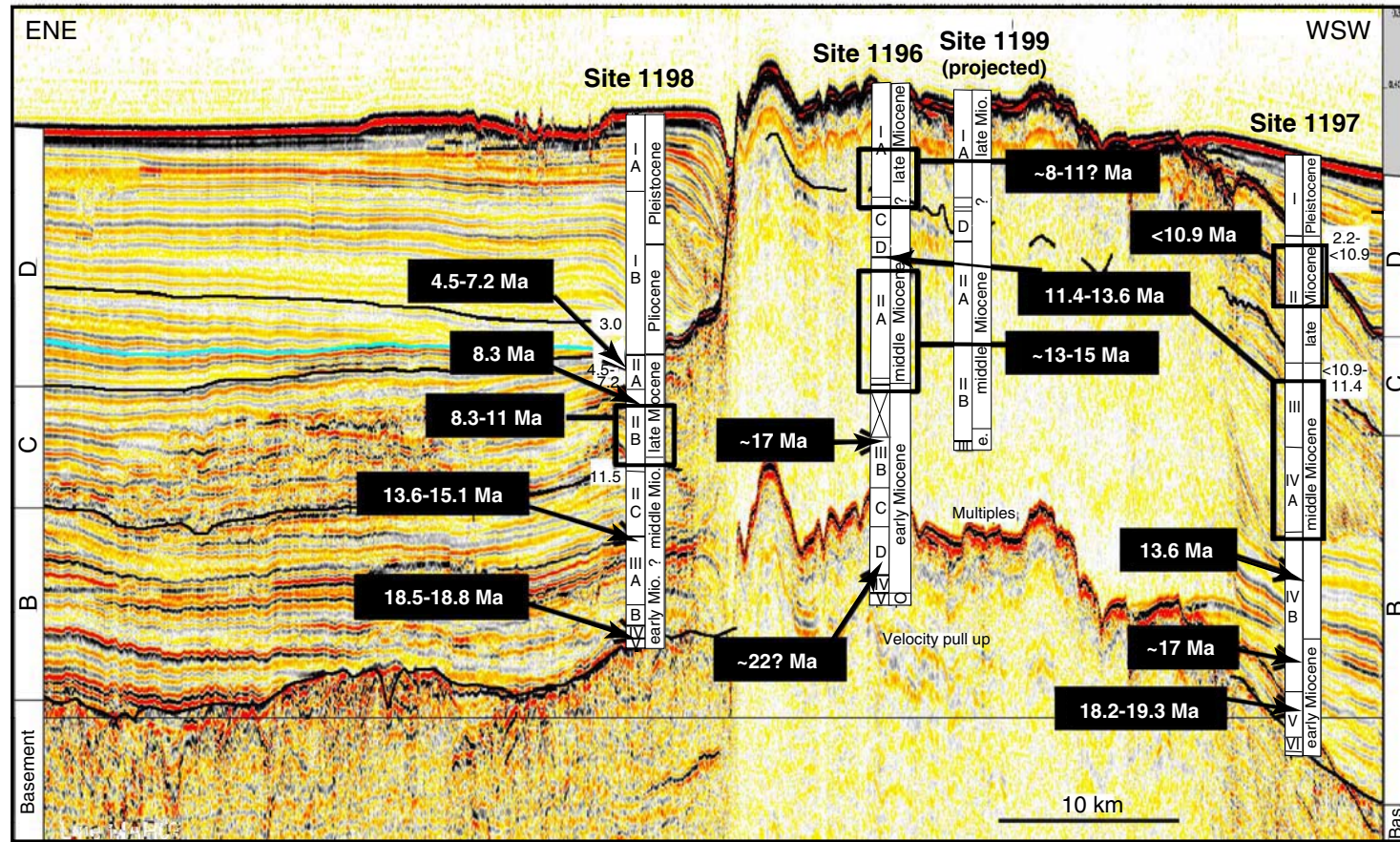
Figure F4. *Operculina complanata* (Op), oyster (Biv) and bryozoan (Bry) fragments, and other bioclastic debris in terrigenous muds from latest Oligocene–earliest Miocene (~22.5 Ma) facies of the Northern Marion Platform (Sample 194-1193C-6R-CC, 0 cm; scale bar = ~1 mm).
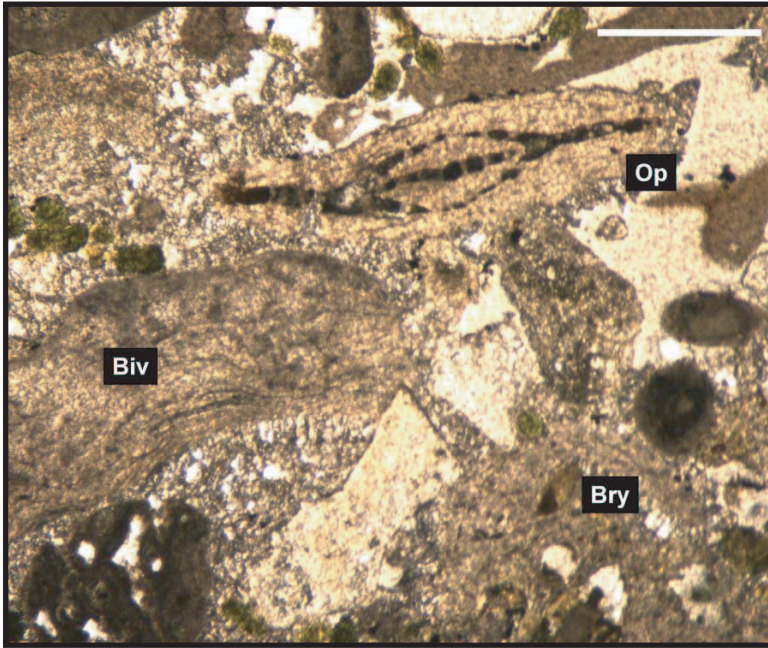
Figure F5. Representative LBF from early Miocene facies of the Northern Marion Platform. Scale bars = ~1 mm. **A**. *Lepidocyclina (Eulepidina) ephippioides* (Le) (Sample 194-1193A-80X-1, 24 cm; ~20.6–22 Ma). **B**. *Cycloclypeus* (Cy), *Lepidocyclina (Nephrolepidina) sumatrensis* (Ln), and *Operculina complanata* (O) (Sample 194-1195B-55X-CC, 12 cm; >20.6 Ma). **C**. *Lepidocyclina (Nephrolepidina) sumatrensis* (Sample 194-1193A-77X-CC, 0 cm; 18.5–20.6 Ma). **D**. Imbricated lepidocyclinid rudstone (Sample 194-1194B-34R-4, 1 cm; ~19 Ma).
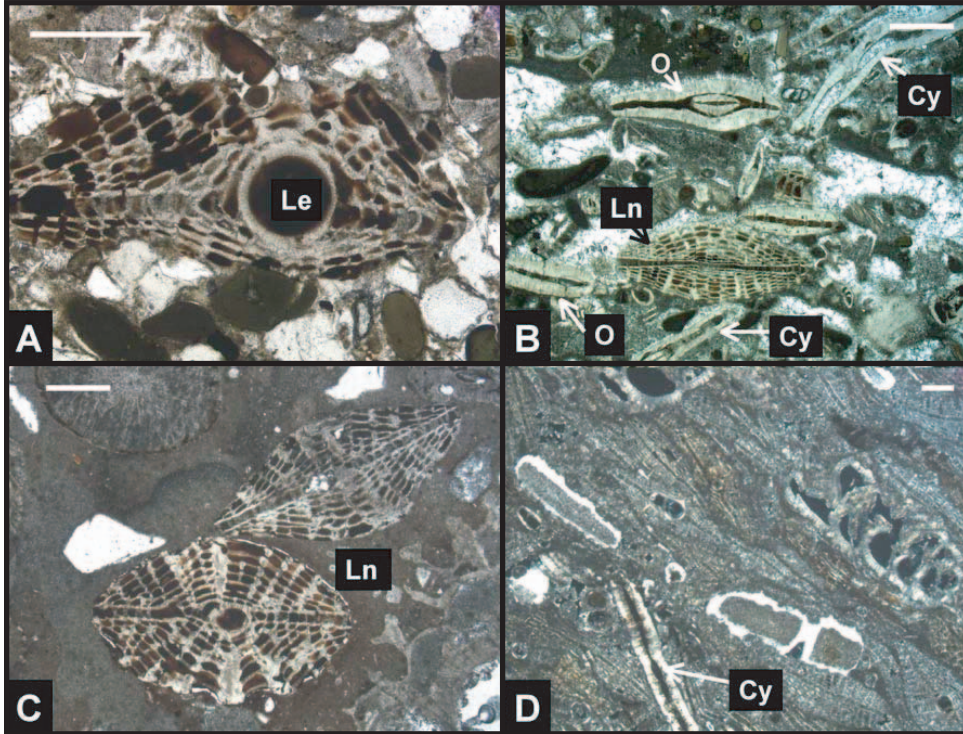
Figure F6. Representative LBF from early Miocene facies of the Southern Marion Platform. Scale bars = ~1 mm. **A**, **B**. *Amphistegina* (Am), *Cycloclypeus* (Cy), *Lepidocyclina* (*Eulepidina*) (Le), *Lepidocyclina* (*Nephrolepidina*) (Ln), and lepidocyclinid fragments (L) in dolomite crystalline matrix. Echinoid plate (E) is also noted (Sample 194-1196A-63R-1, 80 cm; ~22 Ma). **C**. Lepidocyclinids and coralline red algal fragments (R) (Sample 194-1197B-59R-1, 109 cm; 18.2–19.3 Ma). **D**. *Lepidocyclina* (*Eulepidina*) *badjirraensis* (Lb) and coralline red algal fragments (Sample 194-1198B-33R-1, 97 cm; 18.5–18.8 Ma).
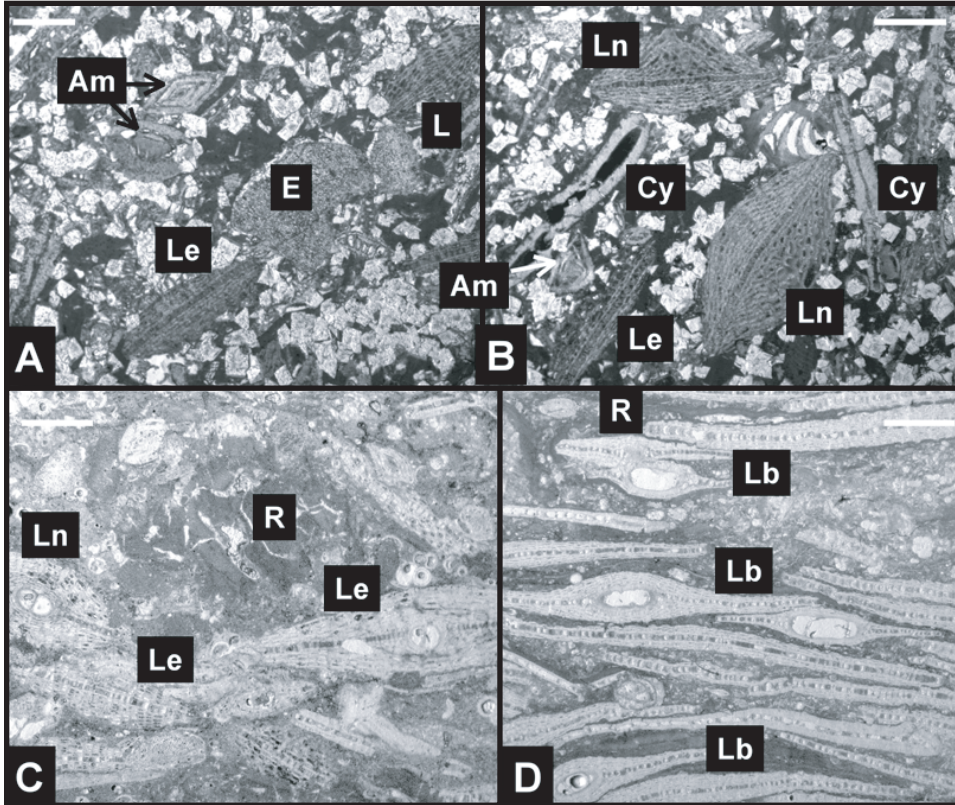
Figure F7. Representative LBF from early Miocene facies of the Northern Marion Platform (Sample 194-1193A-63X-1, 31 cm; 16.8–18.2 Ma [scale bars = ~1 mm]). **A.** *Lepidocyclina* (*Nephrolepidina*) *praehowchini* (Ln). **B.** *Amphistegina* (Am), *Lepidocyclina* (*Nephrolepidina*) *praehowchini* (Ln), bryozoans (Bry), and *Miogypsina* sp. (M; circled). **C.** *Amphistegina* (Am), bryozoans (Bry), echinoids (E) in the lepidocyclinid rudstone matrix, and *Miogypsina* sp. (M; circled). **D.** *Amphistegina* (Am), *Lepidocyclina* (*Nephrolepidina*) *praehowchini* (Ln), and *Cycloclypeus* (Cy).
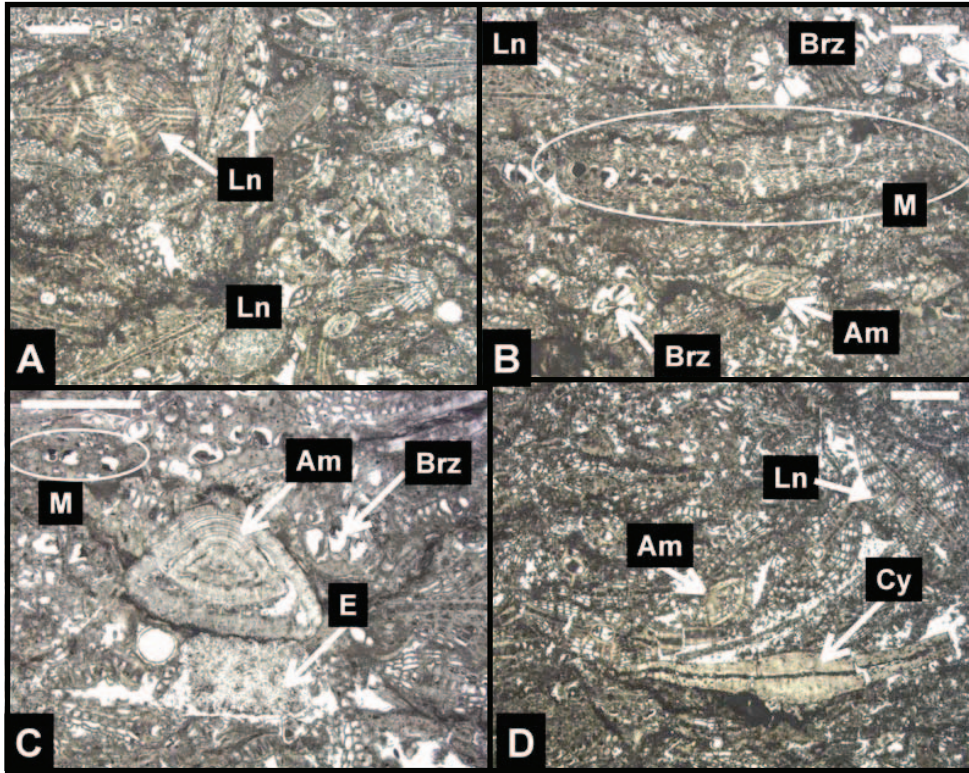
Figure F8. Earliest–middle Miocene (~16.4 Ma) bioclastic debris (Sample 194-1193A-52X-2, 25 cm). R = coralline red algal fragment, B = smaller benthic foraminifer, P = planktonic foraminifer, Ln = *Lepidocyclina* (*Nephrolepidina*) *howchini*?.
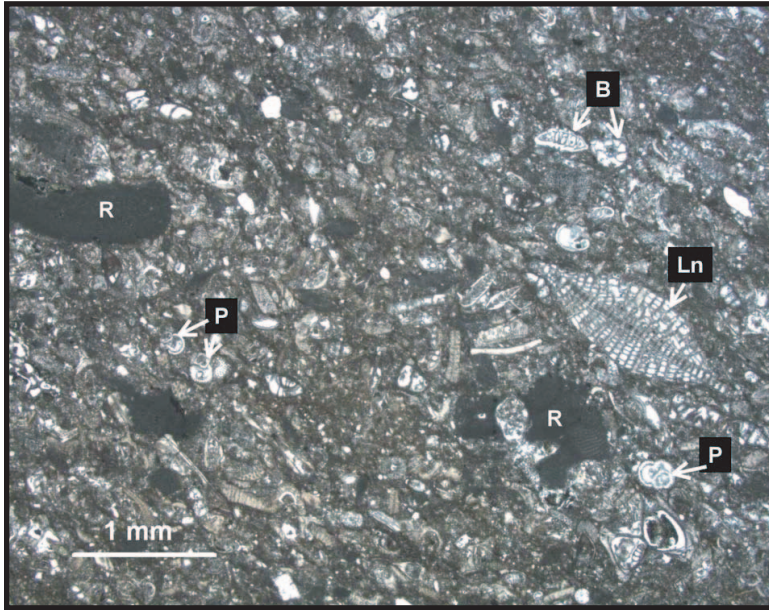
Figure F9. Early to early middle Miocene LBF-rich facies with *Amphistegina* (Am), *Lepidocyclina* (L), *Miogypsina* (M), *Cycloclypeus* (Cy), planktonic foraminifers (P), echinoid plates (E), and coralline red algal fragments (R). Scale bars = ~1 mm. **A, B**. Sample 194-1196A-42R-1, 7 cm. **C**. Sample 194-1197B-53R-5, 92 cm (13.6–18.2 Ma). **D**. Sample 194-1198B-26R-5, 48 cm (15.1–18.5? Ma).
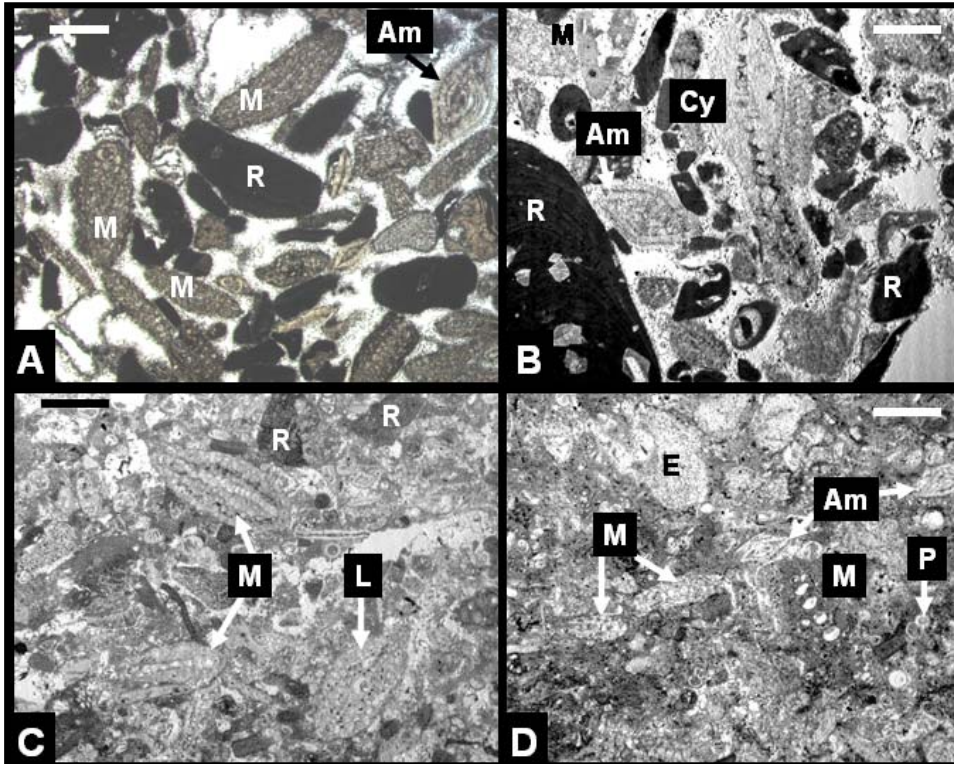
Figure F10. Middle Miocene (11.9–16.4 Ma) LBF-rich facies from Site 1193 with *Amphistegina* (Am), *Cycloclypeus* (Cy), *Lepidocyclina* (*Eulepidina*) fragments (Le), *Lepidocyclina* (*Nephrolepidina*) *howchini* (Lh), *Operculina* (Op), and bryozoan (Bry) and coralline red algal fragments (R). Scale bars = ~1 mm. **A**. Sample 194-1193A-40X-1, 17 cm. **B**. Sample 194-1193A-19X-CC, 5 cm. Very flat, delicate *Cycloclypeus* are indicative of deposition in the oligophotic zone (~100–150 m). **C**. Sample 194-1193A-16X-1, 16 cm (13.6–18.2 Ma). **D**. Sample 194-1193A-12X-1, 6 cm.
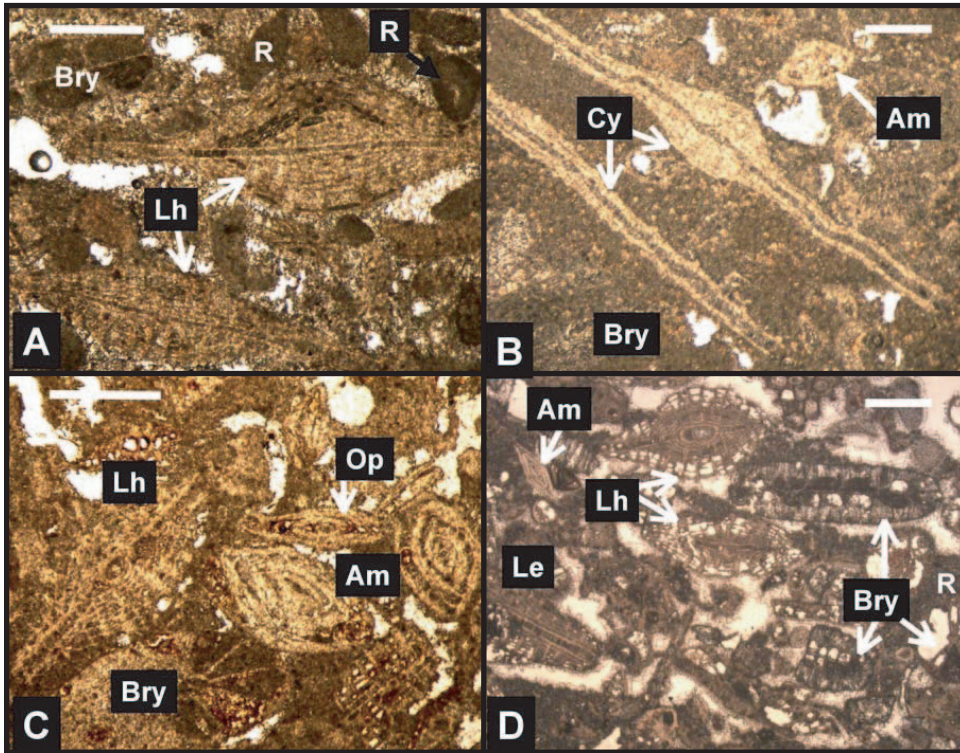
Figure F11. Assemblage interpreted to have lived at ~30–50 m paleodepth, including *Amphistegina "lessonii"* (Al), *Amphistegina "radiata" (Ar)*, and *Operculina complanata* (Op) (Sample 194-1194A-16X-CC, 19 cm). Scale bars = ~1 mm. **A.** Light micrograph of loose specimens. **B.** Thin section.
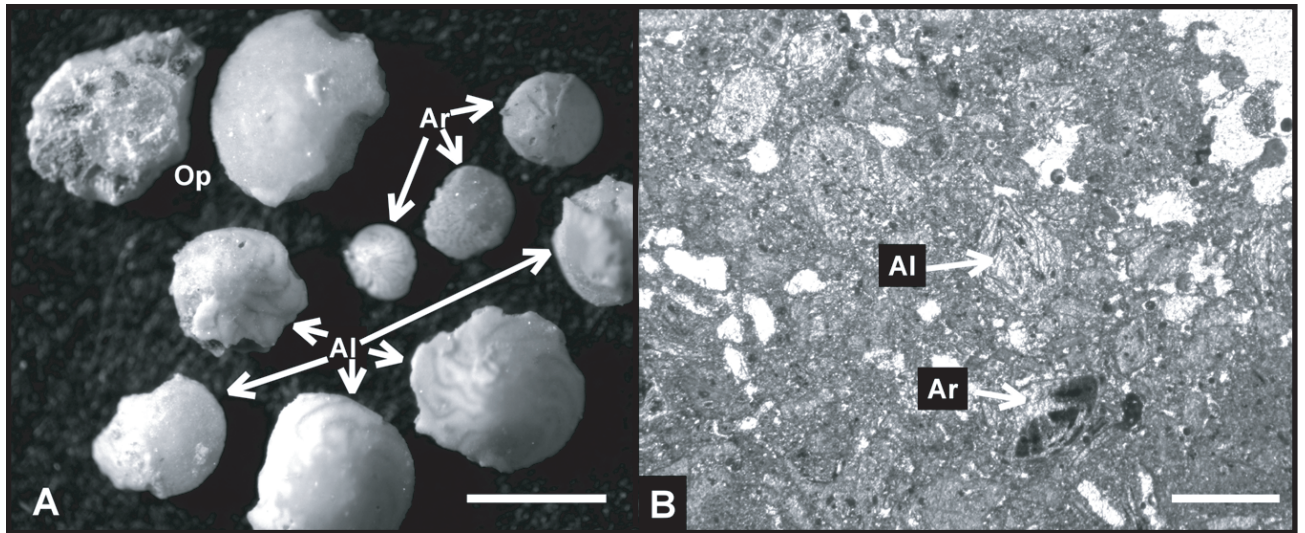
Figure F12. Distinctive foraminifers of the shallow-water facies found between 182 and 336 mbsf at Site 1196, including an unidentified archaiasine (Arc), *Austrotrillina howchini* (Ast), *Flosculinella botangensis* (Flos), *Marginopora* (Mar), and an unidentified soritine (Sor). A gastropod (G) and bivalve shells (Biv) are also evident. Scale bars = ~1 mm. **A, B.** Sample 194-1196A-20R-1, 57 cm. **C.** Sample 194-1196A-33R-1, 19 cm. **D.** Sample 194-1196A-34R-1, 123 cm.
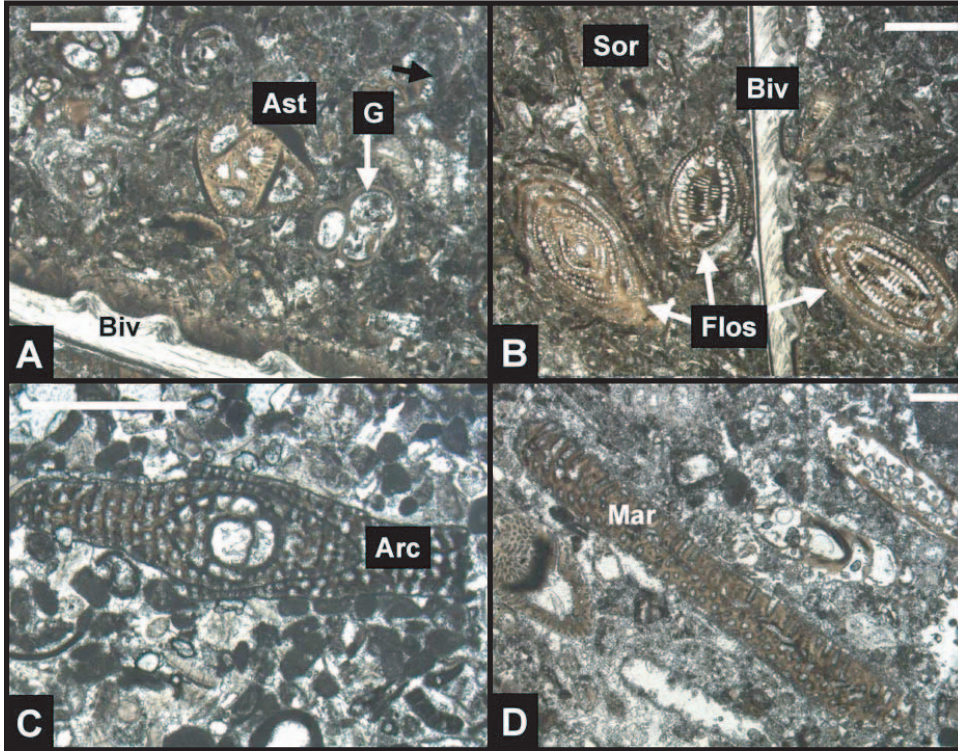
Figure F13. **A**. *Amphistegina* (Am) and a stellate *Lepidocyclina* (L) in a matrix of planktic foraminifers (Sample 194-1197B-38R-5, 111 cm; 13.6 Ma). **B**. *Miogyopsina thecideaeformis* (M) in a matrix of planktonic foraminifers (Sample 194-1198B-20R-2, 9 cm; 13.6–15.1 Ma). **C**, **D**. Mixed LBF assemblage including *Cycloclypeus* (Cy), *M. thecideaeformis*, *Lepidocyclina (Nephrolepidina) howchini* (Lh), and lepidocyclinid fragments (Sample 194-1196A-19R-1, 1 cm).
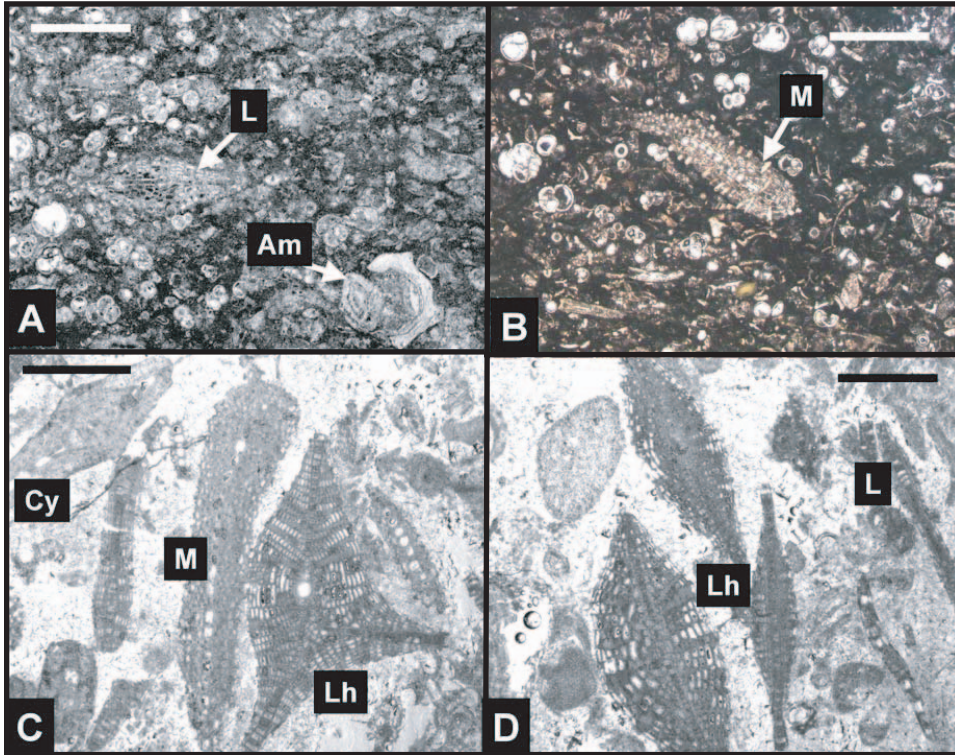
Figure F14. Diverse LBF debris in slope sediments at Site 1197, with *Amphistegina* (Am), *Cycloclypeus* (Cy), *Cycloclypeus* (*Katacycloclypeus*) *annulatus* (Ka), *Lepidocyclina* (L; circled specimen is clearly stellate), *Miogypsina* (M), and *Operculina* (Op) (11.4–13.6 Ma). Scale bars = ~1 mm. **A.** Sample 194-1197B-15R-1, 8 cm. **B.** Sample 194-1197B-16R-1, 24 cm. **C.** Sample 194-1197B-21R-1, 2 cm. **D.** Sample 194-1197B-32R-1, 121 cm.
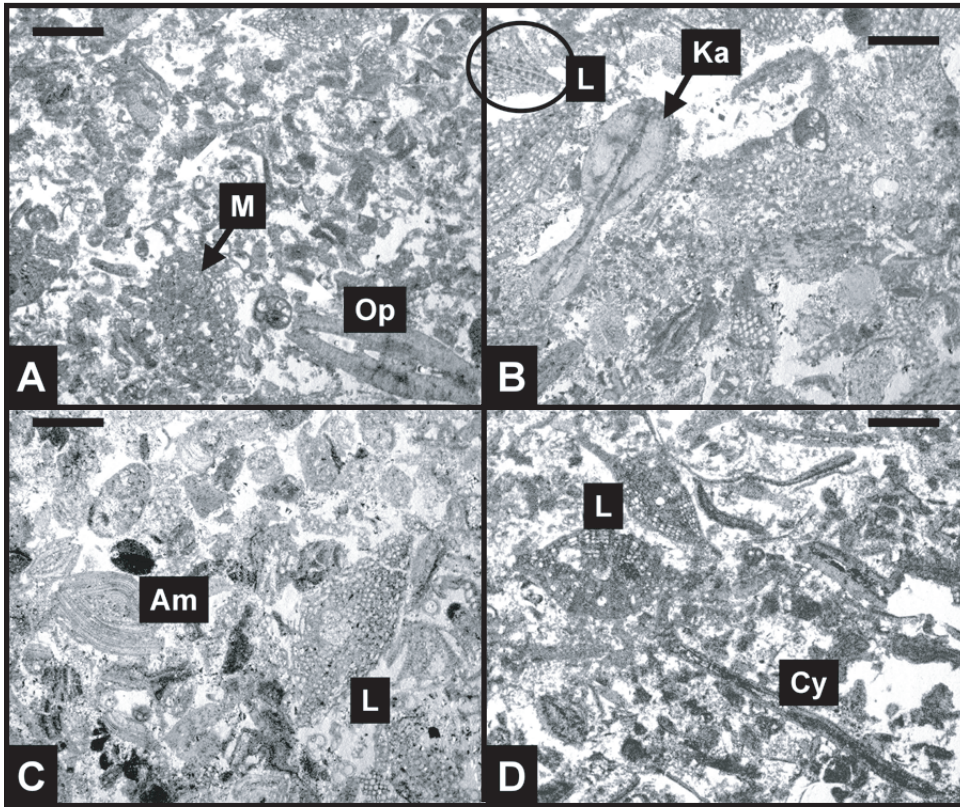
Figure F15. LBF debris in late Miocene slope sediments at Site 1198, with *Amphistegina* (Am), *Cycloclypeus* (Cy), *Lepidocyclina* (L), and planktonic foraminifers (P). Scale bars = 1 mm. **A**. Sample 194-1198B-5R-1, 15 cm (8.3 Ma). **B**. Sample 194-1198B-7R-1, 53 cm (8.3–9 Ma). **C**. Sample 194-1198B-10R-1, 27 cm (9 Ma). **D**. Sample 194-1198B-11R-1, 11 cm (9–11 Ma).
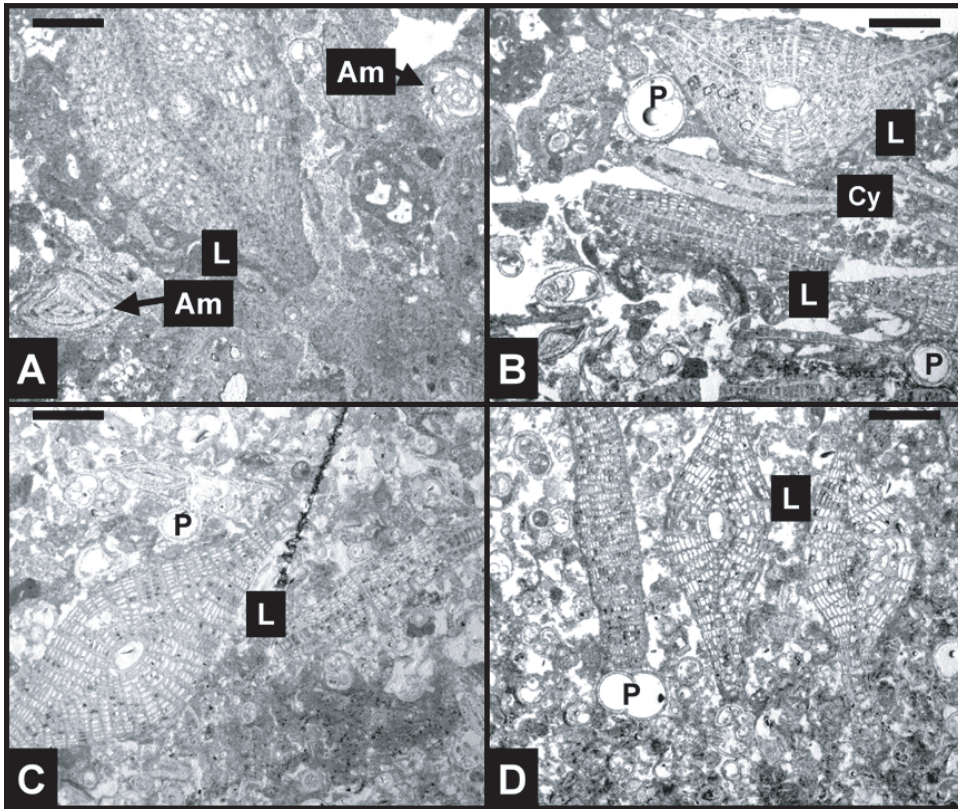
Figure F16. Transported stellate *Lepidocyclina* (Ls) in late Miocene periplatform sediments. Probable *Amphistegina* mold (Am), bryozoan fragment (Bry), *Cycloclypeus* fragment (Cy), echinoid plate (E), partly preserved lepidocyclinids (L), and planktonic foraminifers (P) are also noted. Scale bars = ~1 mm. **A**, **B**. Mud matrix in Sample 194-1193A-5H-1, 143 cm. **C**. Mud matrix in Sample 194-1194B-2R-4, 69 cm. **D**. Porous crystalline matrix in Sample 194-1197B-2R-1, 42 cm.
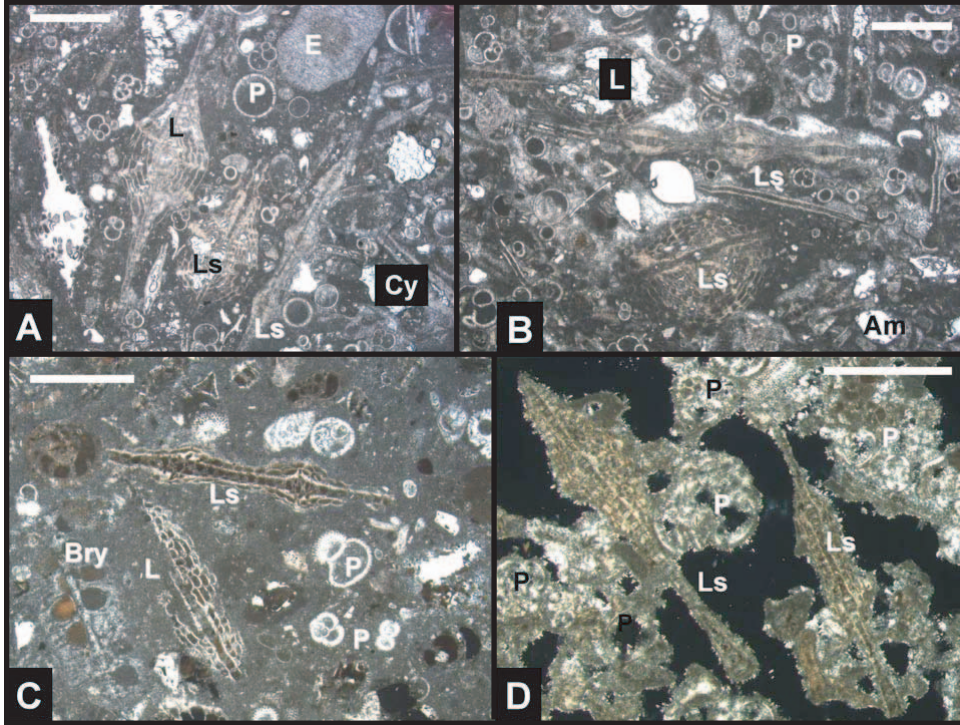
Figure F17. A, B. *Amphistegina* (Am) and stellate *Lepidocyclina* (L) in platform-top sediments (Sample 194-1196A-4R-1, 73 cm). *Cycloclypeus* fragments (Cy), coral fragment (Co), coralline red algal clasts (R), and planktonic foraminifer (P) are also noted. **C, D**. Similar biota in transported sediments (Sample 194-1198B-4R-1, 47 cm; 8.3 Ma). Scale bars = ~1 mm.
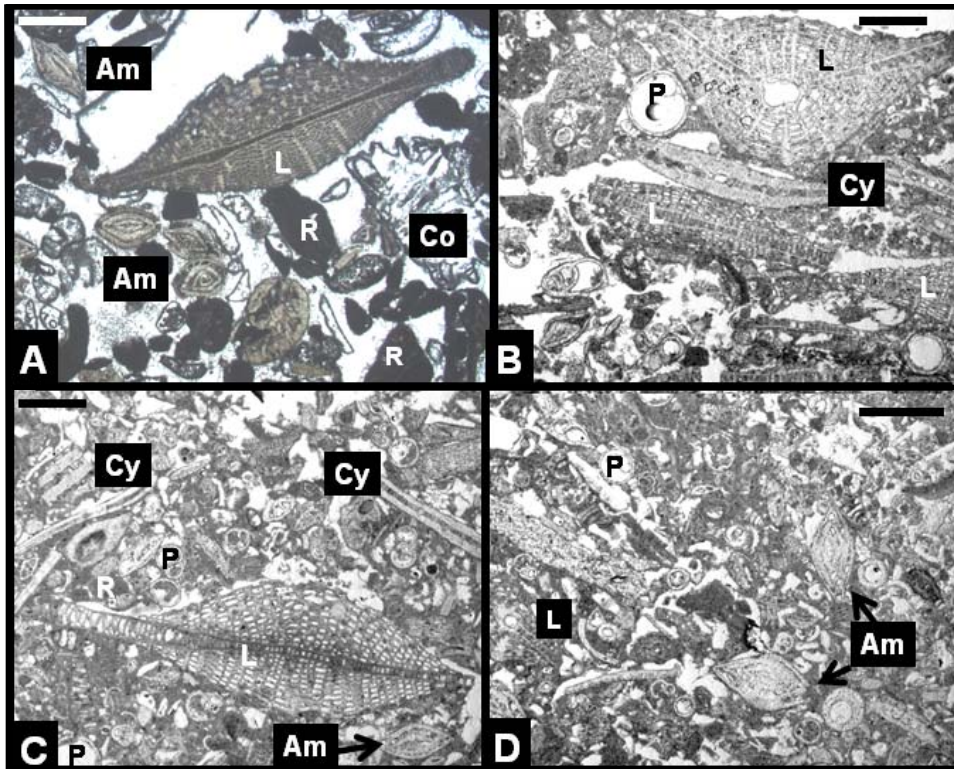
Figure F18. Correlation among Leg 194 drill sites on the northern platform and adjacent slope of the Marion Plateau, with intervals characterized by LBF Assemblages A–E (defined in text) noted. Ages were determined shipboard using nannofossils or planktonic foraminifers (adapted from Shipboard Scientific Party, 2002).
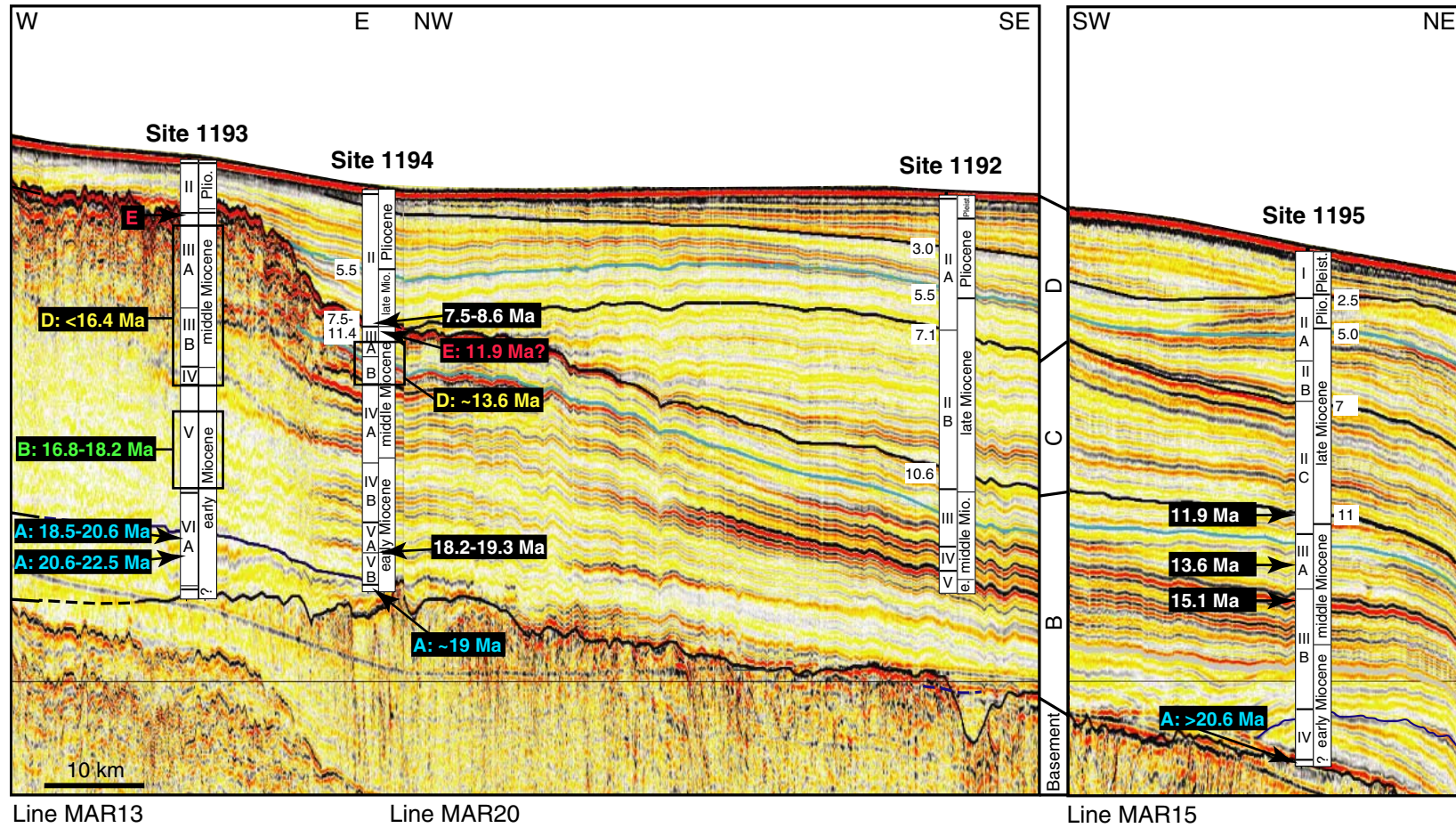
Figure F19. Correlation among Leg 194 drill sites on the southern platform and adjacent slopes of the Marion Plateau, with intervals characterized by LBF Assemblages A–E (defined in text) noted. Ages were determined shipboard, primarily using nannofossils or planktonic foraminifers (adapted from Shipboard Scientific Party, 2002).